

Carbonation front in cement paste detected by T_2 NMR measurements using a low field unilateral magnet

P. F. de J. Cano-Barrita  · B. J. Balcom · F. Castellanos

Received: 21 September 2016 / Accepted: 24 February 2017 / Published online: 7 March 2017
© RILEM 2017

Abstract Unilateral magnetic resonance was used to obtain the CPMG T_2 decay at different positions along 6 cm long cement paste samples. The aim was to detect the carbonation front based on changes in the pore structure caused by accelerated carbonation and to compare the results with the phenolphthalein test. Cement pastes at water-to-cement ratios of 0.60, 0.50, and 0.40 were prepared using ordinary Portland cement. After moist curing and conditioning at 65% RH and 35 °C, the pastes were subjected to accelerated carbonation with 4% by volume CO_2 at 65% RH and 35 °C. Carbonation increases the magnetic resonance T_2 lifetime compared with the control and compared with the noncarbonated region of the samples. A reduction in porosity and changes in the pore size distribution are caused by carbonation. The position with the highest rate of T_2 change was consistent with the fully carbonated front determined by the phenolphthalein test.

Keywords Carbonation · Magnetic resonance · Cement paste · T_2 relaxation time · Pore size distribution · BET

1 Introduction

Carbonation of concrete results from the chemical reaction of CO_2 with calcium hydroxide (CH) and calcium silicate hydrate (CSH), the main cement hydration products. Carbonation is a surface driven process since CO_2 in air diffuses into the concrete cover. Carbonation reduces the pH of the pore solution from 12.6–13.5 to <9 [1]. This negatively affects the protection of the reinforcing steel provided by a thin passivating layer of oxide formed on the steel surface.

Carbonation also reduces the total porosity of ordinary Portland cement (OPC) and alters the pore size distribution. The volume of calcium carbonate formed is 11–12% greater than the specific volume of calcium hydroxide. A reduction in total porosity increases the strength and brittleness of concrete [2]. Ngala and Page [3] found that upon carbonation the proportion of large pores (diameter > 30 nm) increased only slightly for OPC, but was more significant for pastes containing fly ash and slag. In these blended cement pastes where CH is consumed by pozzolanic reactions, carbonation of CSH plays a significant role. Carbonation affects the CSH even at low CO_2 concentrations by producing a porous silica gel with a very coarse pore structure. The silica gel

P. F. de J. Cano-Barrita · B. J. Balcom
Department of Physics, MRI Center, University of New Brunswick, P.O. Box 4400, Fredericton, NB E3B 5A3, Canada

P. F. de J. Cano-Barrita (✉) · F. Castellanos
Instituto Politecnico Nacional-CIIDIR Unidad Oaxaca,
Hornos No. 1003, C.P. 71230 Santa Cruz Xoxocotlán,
Oaxaca, Mexico
e-mail: pcano@ipn.mx

pores are approximately 300 nm in radius [4]. Therefore, the combined effect of carbonation of CH and CSH is a reduction of total porosity and coarsening of the pore structure [3].

The principal technique used to determine the carbonation depth, in the laboratory or in the field, is to spray a phenolphthalein solution over a freshly broken concrete surface [5]. Phenolphthalein, a pH indicator, marks the depth of carbonation through a color change. However, since the colour change occurs at $\text{pH} = 8.6$, it underestimates the carbonation depth. Previous research using thermogravimetric analysis (TGA), powder X-ray diffraction (XRD), and Fourier Transform Infrared Spectroscopy (FTIR) has identified three spatial regions associated with carbonation, carbonated, transition or partially carbonated, and noncarbonated. It has been suggested that the fully carbonated depth (indicated by the phenolphthalein technique) is approximately half the depth of the leading carbonation front (fully + partially carbonated zones) measured by TGA, XRD or FTIR [6].

Nuclear magnetic resonance (NMR) is a non-destructive technique that has been used to study moisture movement in cement-based materials during drying [7] and water absorption [8], as well as to observe chloride and sodium ion penetration [9]. NMR has also been used to observe changes in the pore space of hydrated cement pastes [10–12]. The development of portable [13–17] and embedded [18, 19] NMR devices allows measurements of samples in the laboratory or in field structures. Assuming the fast diffusion limit (e.g. pores are small and the surface relaxation is slow such that a water molecule crosses the pore several times before relaxing [20]), the NMR transverse relaxation rate of pore water in a hydrated cement paste is given by Eq. 1 [12].

$$\frac{1}{T_2} = \rho_2 \frac{S}{V} \quad (1)$$

where $1/T_2$ is the relaxation rate, ρ_2 is the surface relaxivity, and S/V is the surface to volume ratio of the pore space. The surface relaxivity is dependent upon the chemical composition of the solid interacting with pore water molecules.

In this paper T_2 NMR relaxation times are measured with a three-magnet array unilateral NMR device to detect changes in porosity, pore size distribution, and the carbonation depth penetration in cement paste samples subjected to accelerated carbonation in a 4%

Table 1 Cement chemical composition

Oxide	Mass (%)
SiO ₂	21.07
Al ₂ O ₃	3.69
Fe ₂ O ₃	4.50
CaO	61.93
MgO	1.83
Na ₂ O	0.09
K ₂ O	0.30
SO ₃	2.54
LOI	4.38

by volume CO₂ environment at 65% RH and 35 °C. A comparison is given to results with the carbonation front detected with the phenolphthalein test. The T_2 lifetime distribution, which is a proxy for the pore size distribution, is also compared to BET pore size distribution measurements.

2 Materials and method

Cement pastes were prepared with ordinary Portland cement (Table 1) at water to cement (w/c) ratios of 0.40, 0.50, and 0.60. Cylindrical samples 65 mm in diameter and 60 mm in length were cast in plastic containers, sealed and rotated continuously for the first 24 h at about seven rpm using a home-made device to minimize segregation. After 24 h, the samples were stripped and moist cured in saturated limewater for 90 days at 23 °C to reduce the effects of continued hydration on the NMR measurements during carbonation. The saturated samples were cut longitudinally in four parts and conditioned at 65% RH and 35 °C until constant mass was achieved. Since all samples were conditioned under the same environment before carbonation commenced, any drying shrinkage cracking that may occur would affect to the same extent control samples and samples for carbonation. Epoxy resin was applied to all surfaces, except one of the ends. Samples were exposed for 56 days to an automatically controlled 4% by volume CO₂ environment at 65% RH and 35 °C. The relative humidity of 65% was selected to produce a high carbonation rate [1]. Carbonation penetrated the sample from the uncoated end. Control samples were maintained at the same temperature but inside a sealed plastic bag to avoid carbonation.



At 56 days of carbonation the samples were tested with a unilateral three-magnet array (Fig. 1) [13]. The RF probe, a surface coil tuned to a frequency of 4.46 MHz for ^1H was connected to a LapNMR console (Tecmag, Houston, USA) with a 250 W RF amplifier (Tomco Technologies, Stepney, Australia). The transverse magnetization decay was measured with the Carr–Purcell–Meiboom–Gill (CPMG) technique [21]. The samples were displaced longitudinally in steps of 1 cm (measured from the carbonating face) over the center of the surface coil (Fig. 1). The RF probe in combination with the magnet topology yields a measurement spot of approximately 1 cm^3 volume displaced 1 cm from the face of the magnet. Because of the low NMR signal in the samples studied, they were then vacuum saturated with distilled water for 24 h and retested. Vacuum saturation is the recommended technique to ensure that all the pores in cement-based materials are filled with water [22–24]. The CPMG measurement parameters were pulse width = 11 μs , echo time = 170 μs , number of echoes = 256 for samples with $w/c = 0.60$, number of echoes = 128 for samples with w/c ratios of 0.50 and 0.40, number of scans = 2048, for a measurement time of 34 min per displacement. The CPMG decays were fitted to a bi-exponential decay function (Eq. 2) to determine the T_2 lifetimes and their associated signal intensities.

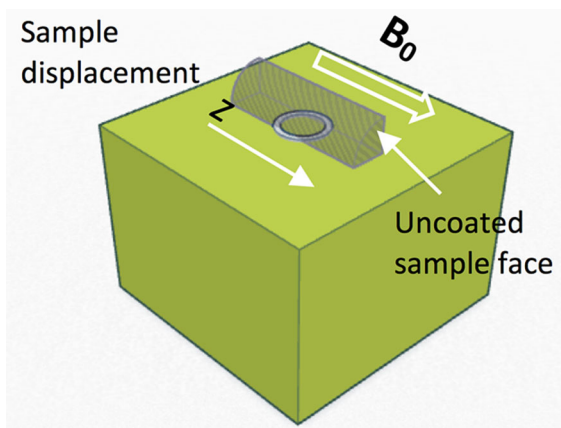


Fig. 1 Unilateral three-magnet array with surface coil tuned at a frequency of 4.46 MHz. The 6 cm long cement paste samples were displaced in steps of 1 cm in the direction indicated by the arrow, each position coinciding with the center of the surface RF coil. The cement paste samples were sealed with epoxy resin on all surfaces, except one face subjected to accelerated carbonation at 4% CO_2 by volume, 65% RH and 35 °C

$$S(t) = M_{0,1} \exp\left(-\frac{t}{T_{2,1}}\right) + M_{0,2} \exp\left(-\frac{t}{T_{2,2}}\right) \quad (2)$$

where S is the signal intensity, $M_{0,1}$ and $M_{0,2}$ are the equilibrium sample magnetization components corresponding to the $T_{2,1}$ and $T_{2,2}$ lifetime constants.

The CPMG decays at carbonated (1 cm) and noncarbonated (5 cm) regions of the vacuum saturated samples were processed by Inverse Laplace Transformation (ILT) to obtain the T_2 distribution, which is considered a proxy for the pore size distribution.

After testing, the samples were fractured in the longitudinal direction and the freshly exposed surface was immediately sprayed with a 1% phenolphthalein solution to estimate the carbonation depth [5]. Samples from one specimen $w/c = 0.60$ and one with $w/c = 0.50$ at carbonated and noncarbonated regions were taken for N_2 BET analysis to obtain the pore size distribution and the pore surface area. The samples were dried for 24 h at 105 °C to eliminate the evaporable water. N_2 adsorption isotherms of the samples were measured using a Belsorp-Max instrument (BEL JAPAN, INC., Osaka, Japan). The adsorption isotherms were measured at 77 K in the relative pressure range $p/p_0 = 10^{-8}$ –0.997. Carbonated and noncarbonated vacuum-saturated samples were measured to determine porosity on a volume basis.

3 Results and discussion

Figure 2 shows typical CPMG decays of a cement paste sample ($w/c = 0.60$), obtained after the carbonation process (Fig. 2a) and after vacuum saturation with distilled water (Fig. 2b). According to the Kelvin equation [25], when the sample is in equilibrium with ambient conditions at 65% RH and 35 °C, pores with a radius larger than approximately 2.3 nm will be empty. This means mostly interlayer and gel water would be found in the hydrated cement paste [1]. Figure 2a shows no difference in the CPMG decays in carbonated (1 cm) and non-carbonated (5 cm) regions of the sample, probably due to the low moisture content which gives incomplete pore occupancy. In both cases, the CPMG decays were best fit to a mono-exponential function. The T_2 lifetime of 0.27 ms confirmed the presence of very tightly held water. The signal to noise ratio (SNR) is very low (≈ 40 –50) for the number of scans employed for a reasonable

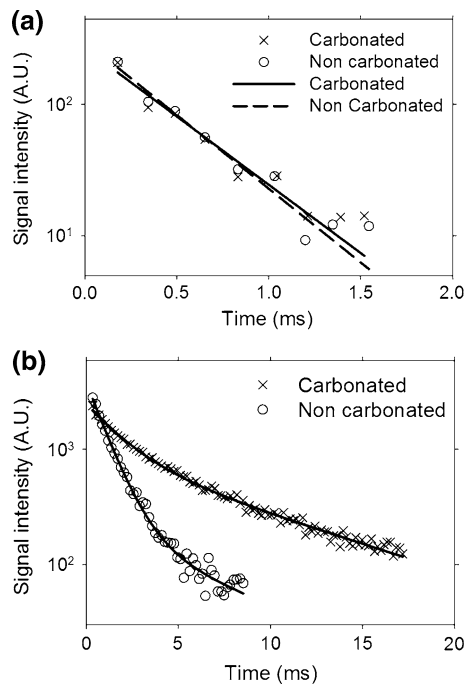


Fig. 2 Semi log plot of the transverse magnetization decay from CPMG measurements for a partially carbonated sample ($w/c = 0.60$) conditioned as follows: **a** in equilibrium with an environment of 65% RH and 35 °C. The SNR of the signal at 1 cm = 43, SNR at 5 cm = 52, and **b** vacuum saturated with distilled water. The SNR of the signal at 1 cm = 209, SNR at 5 cm = 248. The *solid lines* are the best fit to single and bi-exponential decays. The carbonated and noncarbonated signals were obtained at positions 1 and 5 cm from the carbonating face, respectively

measurement time per position. A larger number of scans would improve the SNR but the trends in the behavior would remain unaltered.

Figure 2b shows that after vacuum saturating the sample, which precludes a time-based study, there is a major change in the CPMG decays at the same two positions as reported in Fig. 2a. As expected, the SNR (>200) increases for the same acquisition parameters due to the higher water content. The CPMG measurements now reveal a bi-exponential behavior dominated by the short T_2 lifetime component, which increases in duration in the carbonated region (1 cm) compared to the T_2 lifetime in the noncarbonated region (5 cm). This suggests an increase in pore size of the hydrated cement paste [3, 4] and/or changes in the nature of the pore surface relaxivity [26].

Figure 3 shows the T_2 lifetimes and signal intensities at different positions along samples with three water-to-cement ratios. The T_2 lifetime and signal

intensity values were obtained by fitting the CPMG decays to Eq. 2. The short T_2 lifetime component contributed more than 90% of the total signal intensity. There is a significant increase in the T_2 lifetime where the phenolphthalein test reveals the fully carbonated zone, in comparison with the noncarbonated region. As expected, the T_2 lifetime of the noncarbonated zone is similar to the T_2 lifetime of the control samples. The same trend is observed in cement paste with w/c ratio of 0.50 and to a lesser extent in the paste w/c ratio of 0.40. The sample with w/c ratio of 0.40 seems to be only partially carbonated as the phenolphthalein did not turn completely purple in the outer zone.

Changes in the pore space during cement hydration [19], micro-cracking [27], and autogenous self-healing of cracks [28], are reflected in T_1 and T_2 relaxation times. Since carbonation changes the surface chemistry of the cement paste, the water molecules are now in contact with calcium carbonate particles that may not be as efficient in terms of relaxation as the original noncarbonated surface. The original surface has paramagnetic impurities (Fe_2O_3) which enhance relaxation. Dalas et al. [26] obtained values of the surface relaxivity (ρ_2) of 2.74 and 5.51 $\mu\text{m/s}$ for synthetic calcite and C-S-H, respectively. These values suggest that in our case the observed change in T_2 lifetime may be affected not only by changes in pore size but also by changes in the surface relaxivity. The phenolphthalein test performed after the samples with w/c ratio of 0.60 were characterized by NMR, indicated an average carbonation depth of 2.5 cm. This is in agreement with the observed T_2 lifetime changes in Fig. 3a. These changes are the greatest between 2 and 3 cm, which is a transition zone between the carbonated and noncarbonated regions.

The main advantage of NMR for studying carbonation of cement-based materials compared to traditional techniques is that it is non-destructive. Samples may be studied by bulk or spatially resolved measurements. In this study, limited spatial resolution of the unilateral magnet (1 cm) means it is difficult to determine the actual shape of the carbonation front for the cement pastes with w/c ratios of 0.50 and 0.40. Improving the resolution to less than 1 cm would be possible by reducing the size or modifying the shape of the surface coil. Other alternative is by reducing the width of the sensitive spot produced by the three-magnet array. If resolution becomes higher, it will be possible to detect more precisely the carbonation front

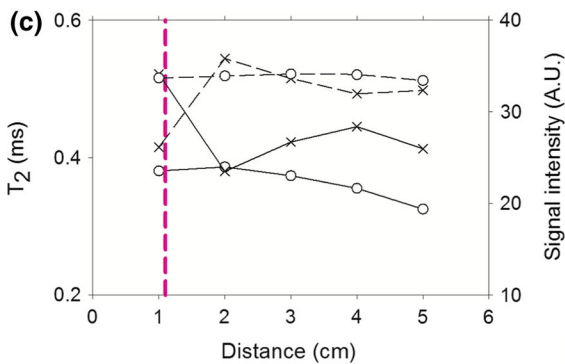
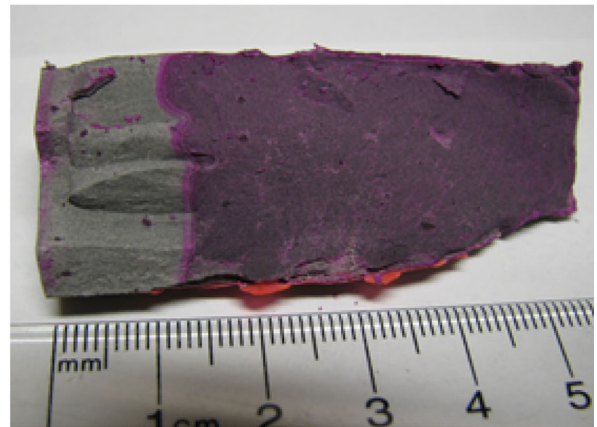
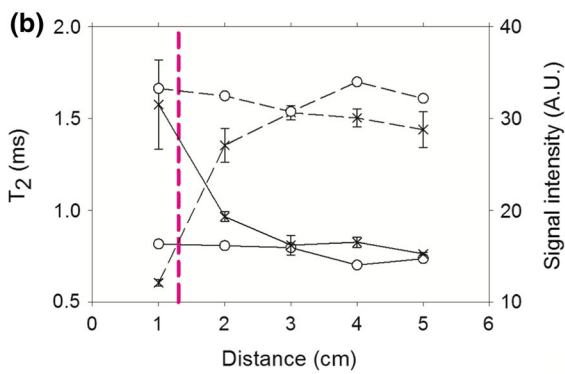
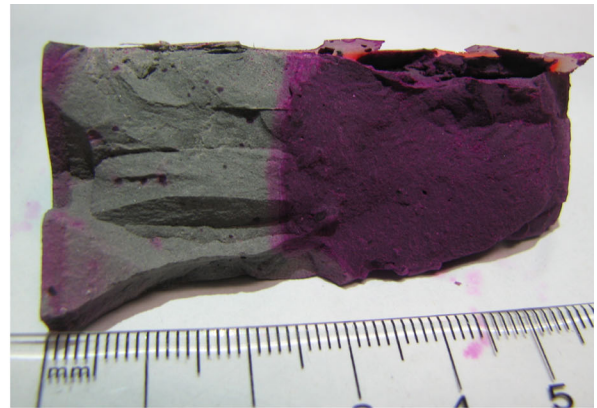
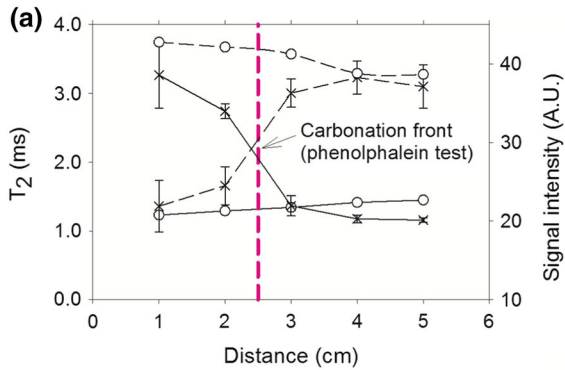


Fig. 3 Long T_2 lifetime component (solid line) and signal intensity (dashed line) versus distance in 6 cm long carbonated (cross) and control (circle) Portland cement pastes. **a** $w/c = 0.60$, **b** $w/c = 0.50$, and **c** $w/c = 0.40$. The samples were vacuum saturated after carbonation in an environment at 4% CO_2 by volume, 65% RH and 35 °C. Photographs to the right indicate the carbonation front after spraying the freshly broken

surface with a 1% phenolphthalein solution. Carbonation front moves from left to right. For the sample $w/c = 0.40$, the carbonated part to the left did not remain colorless as it is not fully carbonated. The error bars indicate one standard deviation for every data point. One control sample was tested for each w/c ratio

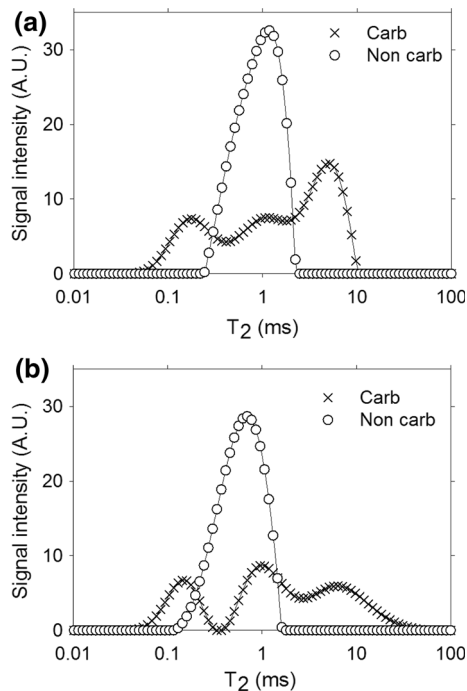


Fig. 4 T_2 distributions obtained by ILT of the CPMG decays for vacuum saturated cement paste samples. **a** $w/c = 0.60$, and **b** $w/c = 0.50$. The positions for carbonated and noncarbonated regions of the sample are points 1 and 5 cm, respectively

in low permeability materials (i.e. low water to cement ratio). For paste with a w/c of 0.60, as mentioned, there is a transition zone that is in agreement with the results obtained by Chang and Chen [6] using TGA, XRD, and FTIR. Their investigations allowed identification of three zones: fully carbonated, partially carbonated, and noncarbonated. They found the fully + partially carbonated zones extended approximately twice the depth indicated by the phenolphthalein test.

The initial CPMG signal intensity is proportional to the amount of water in the sample. Figure 3 also presents the signal intensity at various points along the sample. Contrary to the behavior observed in the T_2 lifetime, the signal intensity (water content) in the carbonated zone is lower than the signal in the noncarbonated zone. This means a lower porosity of the cement paste caused by carbonation, as expected. In ordinary Portland cement pastes, carbonation reduces the total porosity by less than 10% while slightly increasing the proportion of large pores (diameter > 30 nm) [3]. The latter partially supports the increase in T_2 in the carbonated region observed in Fig. 3. It is known that carbonation not only affects the

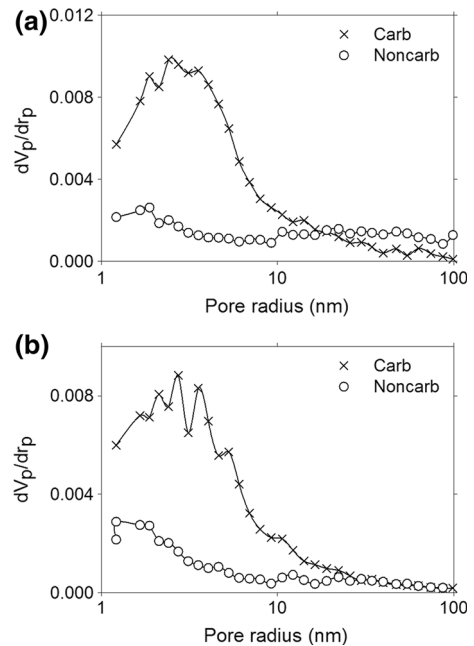


Fig. 5 BET pore size distribution for cement paste samples. **a** $w/c = 0.60$, and **b** $w/c = 0.50$. The symbols indicate: cross carbonated, circle noncarbonated regions

calcium hydroxide in the hydrated cement paste, but it also affects the CSH. A silica gel with a coarser pore structure, pores approximately 300 nm in radius, is produced when the CSH undergoes carbonation [4]. For the three w/c ratios, the CPMG signal intensity in the noncarbonated region is similar to the signal intensity of the control samples.

Figure 4 presents the T_2 distribution obtained by Inverse Laplace Transformation of the CPMG decays in carbonated and noncarbonated zones of the cement paste samples (w/c ratio of 0.60 and 0.50). For CPMG decays with low signal-to-noise ratio, the ILT has shown to be unable to resolve the two peaks commonly reported in the literature for water in gel and capillary pores [16]. This is the case for the noncarbonated sample with low signal-to-noise ratio CPMG decay (see Fig. 2b), where the ILT resolves only one peak that represents an average T_2 from water in all the pores. In both cement pastes, the pore size distribution indicates changes of the pore structure. A refinement of the porosity is observed (short T_2 values) caused by precipitation of CaCO_3 in small pores [29] that contained water during the carbonation period at 65% RH. At the same time, there is an increase of the pore size (long T_2 values) corresponding to the

Table 2 N₂ BET parameters and porosity on a volume basis for carbonated and noncarbonated cement pastes

w/c ratio	BET parameters			Porosity (%)
	Mean pore radius (nm)	Surface area (m ² /g)	Pore volume (cm ³ /g)	
0.60 carbonated	2.4	37	0.112	43
0.60 noncarbonated	1.9	14	0.128	49
0.50 carbonated	2.7	32	0.087	37
0.50 noncarbonated	1.2	10	0.040	46

amorphous silica gel produced by carbonation of the CSH [4]. However, the porosity is reduced as shown by the smaller area under the curves for the carbonated zones in comparison with the noncarbonated parts of the samples. Thiery et al. [30] measured T_1 relaxation times of carbonated and noncarbonated cement pastes after saturation with liquid water. Contrary to our results, their results showed no difference in T_1 distribution between the carbonated and noncarbonated samples.

In contrast to the results shown in Fig. 4, the pore size distribution obtained by the N₂ BET measurements (Fig. 5) indicates a substantially different pore structure of the carbonated and noncarbonated regions. Regarding the pore size distribution, the carbonated zone in Fig. 5a (paste with w/c = 0.60) exhibits reduction of the pore size in the range of 10–100 nm and an increase of the pore size in the range of 3–10 nm. The paste with w/c ratio = 0.50 indicates increase of the pore size for the carbonated paste. None of the BET pore size distributions show the pores corresponding to the silica gel because the pore size (radius > 300 nm) is outside the range of analysis for this technique. In addition, because the samples were dried at 105 °C for 24 h for BET measurements, micro-cracking and shrinkage changed the pore structure of the cement paste, especially by the collapse of the delicate CSH structure. The NMR measurements did not cause any damage to the samples and provide a more reliable pore structure measurement of the carbonated and noncarbonated samples.

Table 2 shows the BET results and the total porosity for the cement paste samples with w/c ratio of 0.60 and 0.50. The surface area in the carbonated region of the sample was increased nearly three times compared to the noncarbonated sample. This is caused by the large amount of small CaCO₃ particles precipitated in the pore space [31]. Note that the mean pore radius is increased for the carbonated samples. The total porosity for the

noncarbonated cement pastes is within the range of values found in the literature for Portland cement pastes with similar w/c ratios [3, 32]. In addition, the porosity is lower in the carbonated samples, which is also in agreement with the literature [4].

4 Conclusions

Conditioning samples at 65% RH did not provide sufficient NMR signal to detect changes in T_2 lifetime. However, NMR measurements on vacuum saturated samples reveal significant changes in the porosity and the pore size distribution in the carbonated regions of the samples. The observed changes included an increase of T_2 lifetimes and decrease in NMR signal intensity in the carbonated region. The position with the highest rate of T_2 lifetime change is in agreement with the carbonation front indicated by the phenolphthalein test. The T_2 distributions indicated both pore size refinement due to precipitation of CaCO₃ and pore size increase due to porous silica gel formation by carbonation of CSH. The BET results did not agree with the literature nor with the NMR measurements, probably because of the damage cause by oven drying the samples. Unilateral NMR can be used in the laboratory to non-destructively study the carbonation process of cement pastes.

5 Future research

Extension of the measurements to mortars and concrete subject to accelerated and natural carbonation will be pursued in the future.

Acknowledgements P. Cano acknowledges Consejo Nacional de Ciencia y Tecnologia of Mexico (Grant Number 257348) and Instituto Politecnico Nacional of Mexico for the financial support for his sabbatical year at the UNB MRI Centre.



B. J. Balcom thanks NSERC of Canada for a Discovery grant (Grant Number RGPIN-2015-06122) and the Canada Chairs program for a Research Chair in MRI of Materials (Grant Number 950-230894). P. Cano also acknowledges his students and colleagues from CIIDIR Unidad Oaxaca for preparing and carbonating the cement paste samples used for this research.

Compliance with ethical standards

Conflict of interest The authors declare that they have no conflict of interest.

References

- Neville AM (1995) Properties of concrete, 4th edn. Longman Group, Harlow Essex
- Xiao J, Li J, Zhu B, Fan Z (2002) Experimental study on strength and ductility of carbonated concrete elements. *Constr Build Mater* 16:187–192
- Ngala VT, Page CL (1997) Effects of carbonation on pore structure and diffusional properties of hydrated cement pastes. *Cem Concr Res* 27:995–1007
- Bier TA, Kropp J, Hilsdorf HK (1989) The formation of silica gel during carbonation of cementitious systems containing slag cements. In: Proceedings of the 3rd international conference on the use of fly ash, silica fume, slag, and natural pozzolans in concrete, Trondheim, pp 1413–1428
- RILEM Recommendations CPC-18 (1988) Measurement of hardened concrete carbonation depth. *Mater Struct* 21:453–455
- Chang CF, Chen JW (2006) The experimental investigation of concrete carbonation depth. *Cem Concr Res* 36:1760–1767
- Cano-Barrita PF de J, Balcom BJ, Bremner TW et al (2004) Moisture distribution in drying ordinary and high performance concrete cured in a simulated hot dry climate. *Mater Struct* 37:522–531
- Balcom BJ, Barrita JC, Choi C et al (2003) Single-point magnetic resonance imaging (MRI) of cement based materials. *Mater Struct* 36:166–182
- Cano F de J, Bremner TW, MacGregor RP, Balcom BJ (2002) Magnetic resonance imaging of ^1H , ^{23}Na , and ^{35}Cl penetration in Portland cement mortar. *Cem Concr Res* 32:1067–1070
- Bhattacharja S, Moukwa M, D'Orazio F et al (1993) Microstructure determination of cement pastes by NMR and conventional techniques. *Adv Cem Based Mater* 1:67–76
- Jehng JY, Sprague DT, Halperin WP (1996) Pore structure of hydrating cement paste by magnetic resonance relaxation analysis and freezing. *Magn Reson Imaging* 14:785–791
- Halperin WP, Jehng JY, Song YQ (1994) Application of spin-spin relaxation to measurement of surface area and pore size distributions in a hydrating cement paste. *Magn Reson Imaging* 12:169–173
- García-Naranjo JC (2012) Three-magnet arrays for unilateral magnetic resonance. PhD Thesis, University of New Brunswick
- García-Naranjo JC, Guo P, Marica F et al (2014) Magnetic resonance core-plug analysis with the three-magnet array unilateral magnet. *Petrophysics* 55:229–239
- Manz B, Coy A, Dykstra R et al (2006) A mobile one-sided NMR sensor with a homogeneous magnetic field: the NMR-MOLE. *J Magn Reson* 183:25–31
- Boguszynska J, Brown MCA, McDonald PJ et al (2005) Magnetic resonance studies of cement based materials in inhomogeneous magnetic fields. *Cem Concr Res* 35:2033–2040
- McDonald PJ, Aptaker PS, Mitchell J, Mulheron M (2007) A unilateral NMR magnet for sub-structure analysis in the built environment: the Surface GARField. *J Magn Reson* 185:1–11
- Cano-Barrita PF de J, Marble AE, Balcom BJ et al (2009) Embedded NMR sensors to monitor evaporable water loss caused by hydration and drying in Portland cement mortar. *Cem Concr Res* 39:324–328
- Díaz-Díaz F, Cano-Barrita PF de J, Balcom BJ et al (2013) Embedded NMR sensor to monitor compressive strength development and pore size distribution in hydrating concrete. *Sensors* 13:15985–15999
- Coates GR, Xiao L, Prammer MG (1999) NMR logging principles & applications. Halliburton Energy Services, Houston
- Meiboom S, Gill D (1958) Modified spin-echo method for measuring nuclear relaxation times. *Rev Sci Instrum* 29:688–691
- ASTM C 642-13 (2013) Standard test method for density, absorption, and voids in hardened concrete. ASTM International, West Conshohocken
- Bu Y, Spragg R, Weiss WJ (2014) Comparison of the pore volume in concrete as determined using ASTM C642 and vacuum saturation. *Adv Civ Eng Mater* 3:308–315
- Safiuddin M, Hearn N (2005) Comparison of ASTM saturation techniques for measuring the permeable porosity of concrete. *Cem Concr Res* 35:1008–1013
- Bentz DP (2005) Curing with admixtures beyond drying shrinkage reduction. *Concr Int* 27:55–60
- Dalas F, Korb J-P, Pourchet S et al (2014) Surface relaxivity of cement hydrates. *J Phys Chem C* 118:8387–8396
- Beyea SD, Balcom BJ, Bremner TW et al (2003) Detection of drying-induced microcracking in cementitious materials with space-resolved ^1H nuclear magnetic resonance relaxometry. *J Am Ceram Soc* 86:800–805
- Huang H, Ye G, Pel L (2016) New insights into autogenous self-healing in cement paste based on nuclear magnetic resonance (NMR) tests. *Mater Struct* 49:2509–2524
- Šavija B, Luković M (2016) Carbonation of cement paste: understanding, challenges, and opportunities. *Constr Build Mater* 117:285–301
- Thiery M, Faure P, Morandea A et al (2011) Effect of carbonation on the microstructure and the moisture properties of cement-based materials. In: De Freitas VP, Corvacho H, Lacasse MA (eds) XII DBMC international conference on durability of building materials and components. FEUP Edicoes, Porto, pp 1–8
- Talakokula V, Bhalla S, Ball RJ et al (2016) Diagnosis of carbonation induced corrosion initiation and progression in reinforced concrete structures using piezo-impedance transducers. *Sens Actuators A* 242:79–91
- Cook RA, Hover KC (1999) Mercury porosimetry of hardened cement pastes. *Cem Concr Res* 29:933–943

